Inorg. Chem. **2002**, *41*, 6831–6837

Moderating Influence of Proteins on Nonplanar Tetrapyrrole Deformations: Coenzyme F430 in Methyl-Coenzyme-M Reductase

Lindsay N. Todd and Marc Zimmer*

Chemistry Department, Connecticut College, New London, Connecticut 06320

Received August 14, 2002

Normal-coordinate structural decomposition, cluster analysis, and molecular mechanics calculations were undertaken to examine the effect of methyl-coenzyme-M reductase (MCR) on the nonplanar deformations of coenzyme F430. Although free 12,13-diepi-F430 has a lower energy conformation than free F430, the protein restraints exerted by MCR are responsible for F430 having a lower energy conformation than the 12,13-diepimer in MCR. According to the NSD analysis, the crystal structure of free diepimerized F430M is highly distorted. In MCR the protein prevents 12,13-diepi-F430 from undergoing nonplanar deformations; therefore, MCR favors F430 over the 12,13-diepimeric form. The strain imposed on 12,13-diepi-F430 in the protein is so large that although 88% of free F430 is found in the diepimeric form, none of the diepimeric form is found in MCR. This is of significance since the two forms have different chemistries. MCR also moderates the nonplanar deformations of coenzyme F430, which are known to affect redox potentials and axial ligand affinities in tetrapyrroles, suggesting that the protein environment (MCR) is responsible for tuning the chemistry of the active site nickel ion. F430 is bound to MCR by hydrogen bonds between the protein and the F430 carboxylate groups. Conformational searches have shown that F430 has very little rotational and translational freedom within MCR.

Introduction

Proteins can enforce unstable geometries to increase the reactivity of an enzyme's active site. In the case of metalloenzymes this is known as the entatic or rack state. This work shows that methyl-coenzyme-M reductase (MCR) modifies the reactivity of the nickel active site by changing the conformations available to coenzyme F430 in two ways.

MCR. Anaerobic bacteria produce 400 million ton of methane annually. About 45 million metric tons of the methane escape into the troposphere and significantly contribute to the greenhouse effect.[1] MCR is a key enzyme common to all methane-producing pathogens. It catalyzes the last step of methanogenesis in which methyl-coenzyme M (Me-CoM) and coenzyme B are joined by the formation of a disulfide bond (CoM−S−S−CoB), and methane is released (Scheme 1).

Crystal structures of MCR from *Methanobacterium marburgensis*, *Methanosarcina barkeri*, and *Methanopyrus kandleri* have been published.[2−4] Each MCR is composed of three subunits in a $(\alpha\beta\gamma)_2$ structure and contains two noncovalently bound molecules of cofactor F430. This unusual nickel tetrahydrocorphinoid cofactor (Figure 1) is most likely the active site of MCR.[5]

Scheme 1

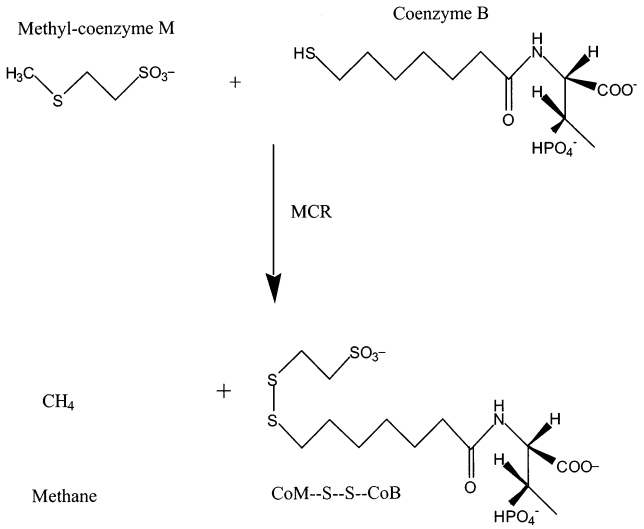

* Author to whom correspondence should be addressed. E-mail: mzim@conncoll.edu.

(1) Ferry, J. G. *Science* **1997**, *278*, 1413.

(2) Grabarse, W.; Mahlert, F.; Duin, E. C.; Goubeaud, M.; Shima, S.; Thauer, R. K.; Lamzin, V.; Ermler, U. *J. Mol. Biol.* **2001**, *309*, 315−330.

10.1021/ic025950v CCC: $22.00
Published on Web 11/12/2002

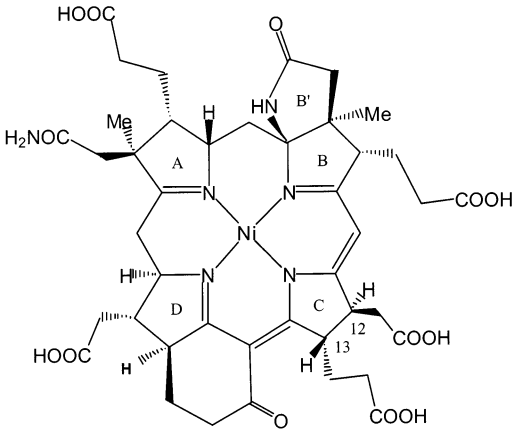

Figure 1. Structure of F430. Diepimerization occurs at positions 12 and 13.

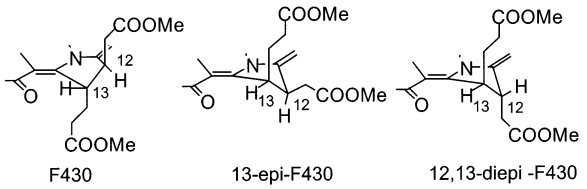

Figure 2. At thermodynamic equilibrium 4% of native F430, 8% of 13-epi-F430, and 88% of the most stable isomer 12,13-diepi-F430 are found.

The F430 is held in place within the protein via hydrogen bonding to the partially negatively charged carboxylate groups of the Ni-porphrinoid.[6] The nickel ion is redox active and is found in nickel(I) EPR visible as well as nickel(II) EPR silent forms.[7−9]

Free F430. Free coenzyme F430 is thermally unstable; it first epimerizes to 13-epi-F430 and then in a second epimerization to 12,13-diepi-F430[10] (Figure 2). Because of problems in the purification procedure, the crystal structure of free F430 has not been solved; however, the structure of a methanolated derivative, 12,13-diepi-F430M, has been published.[11] The corphinoid ring is significantly deformed from planarity. Empirical force-field calculations based on the structure of 12,13-diepi-F430M have been used to show that the diepimeric form of F430 has a smaller hole size (nickel(II)) than the native form of F430 (nickel(I)). These results have been confirmed by subsequent density functional theory (DFT) calculations.[12,13] However, the DFT and empirical force-field calculations predict differing macrocyclic conformations for high-spin nickel(II) F430. DFT calculations predict a planar conformation,[14] while molecular mechanical methods predict that the diepimerization to native F430 will involve a large conformational change from a ruffled geometry to a saddled geometry.[15]

Molecular mechanics calculations of free F430 have also been used to propose that it could adopt a taco-like conformation with trigonal bipyramidal nickel that is not available to the more commonly found porphyrins because of their more extensive conjugation.[16]

To date, all computational analyses of nickel cofactor F430 have used free F430. In this paper we describe the effect of the protein environment on the conformation of F430. Does MCR affect the magnitude of the nonplanar deformations of F430, its epimerization, etc.?

Nonplanar Deformations. At one time it was thought that the aromatic porphyrin macrocycle would be planar. In fact, early structure determinations constrained the macrocycle to be planar. However, when high-quality crystallographic determinations of porphyrins and metalloporphyrins began to appear, it was soon obvious that the porphyrin ring was subject to a number of distortions and was often distinctly nonplanar. The nonplanarity of porphyrins is biologically relevant[17] and influences the chemical properties of porphyrin complexes.

Most deformations of the porphyrin core are in a direction perpendicular to the tetra-aza plane. They can be classified into six classes (Figure 3). These are based on simple symmetric deformations, one of each out-of-plane symmetry classification of the (D_{4h}) point group of the square-planar macrocycle. More complicated asymmetric distortions that are composed of combinations of these simple distortions are also found.

A normal-coordinate structural decomposition (NSD) procedure has been used to characterize and quantify porphyrin deformations in proteins.[17,18] The method determines the out-of-plane distortions in terms of the equivalent distortions along the lowest-frequency normal coordinates of the porphyrin.[19] Prior NSD analyses of porphyrins of protein structures from the Protein Data Bank (pdb) have revealed previously hidden conservation of the nonplanar conformation of the porphyrin for many protein types.[20] For example, *c*-type cytochromes with their covalently bound hemes show a characteristic distortion that is predominately *ruf*, and peroxidases exhibit a predominately *sad* distortion.[21] The conservation of these characteristic macrocycle structures for proteins, which differ in their amino acid sequences but

(3) Grabarse, W. G.; Mahlert, F.; Shima, S.; Thauer, R. K.; Ermler, U. *J. Mol. Biol.* **2000**, *303*, 329−344.
(4) Ermler, U.; Grabarse, W.; Shima, S.; Goubeaud, M.; Thauer, R. K. *Science* **1997**, *278*, 1457−1462.
(5) Pelmenschikov, V.; Blomberg, M. R. A.; Siegbahn, P. E. M.; Crabtree, R. H. *J. Am. Chem. Soc.* **2002**, *124*, 4039−4049.
(6) Ermler, U.; Grabarse, W.; Shima, S.; Goubeaud, M.; Thauer, R. K. *Curr. Opin. Struct. Biol.* **1998**, *8*, 749−758.
(7) Telser, J.; Davydov, R.; Horng, Y. C.; Ragsdale, S. W.; Hoffman, B. M. *J. Am. Chem. Soc.* **2001**, *123*, 5853−5860.
(8) Thauer, R. K. *Microbiology* **1998**, *144*, 2377−2406.
(9) Becker, D. F.; Ragsdale, S. W. *Biochemistry* **1998**, *37*, 2639−2647.
(10) Pfaltz, A.; Jaun, B.; Diekert, G.; Thauer, R. K.; Eschenmoser, A. *Helv. Chim. Acta* **1985**, *68*, 1338−1358.
(11) Faerber, G. K. W.; Kratky, C.; Jaun, B.; Pfaltz, A.; Spinner, C.; Kobelt, A.; Eschenmoser, A. *Helv. Chim. Acta* **1991**, *74*, 697−716.
(12) Ghosh, A.; Wondimagegn, T.; Ryeng, H. *Curr. Opin. Chem. Biol.* **2001**, *5*, 744−750.
(13) Wondimagegn, T.; Ghosh, A. *J. Am. Chem. Soc.* **2000**, *122*, 6375−6381.
(14) Ghosh, A.; Steene, E. *J. Biol. Inorg. Chem.* **2001**, *6*, 739−752.
(15) Zimmer, M. *Journal Biomol. Struct. Dyn.* **1993**, *11*, 203−214.
(16) Zimmer, M.; Crabtree, R. *J. Am. Chem. Soc.* **1990**, *112*, 1062−1066.
(17) *Porphyrin Handbook*; Shelnutt, J. A., Kadish, K. M., Smith, K. M., Guilard, R., Eds.; Academic Press: Boston, 2000.
(18) Shelnutt, J. A.; Song, X. Z.; Ma, J. G.; Jia, S. L.; Jentzen, W.; Medforth, C. J. *Chem. Soc. Rev.* **1998**, *27*, 31−41.
(19) Jentzen, W.; Song, X.; Shelnutt, J. *J. Phys. Chem.* **1997**, *101*, 1684−1699.
(20) Jentzen, W.; Ma, J.-G.; Shelnutt, J. A. *Biophys. J.* **1998**, *74*, 753−763.
(21) Shelnutt, J. A. *J. Porphyrins Phthalocyanines* **2000**, *4*, 386−389.

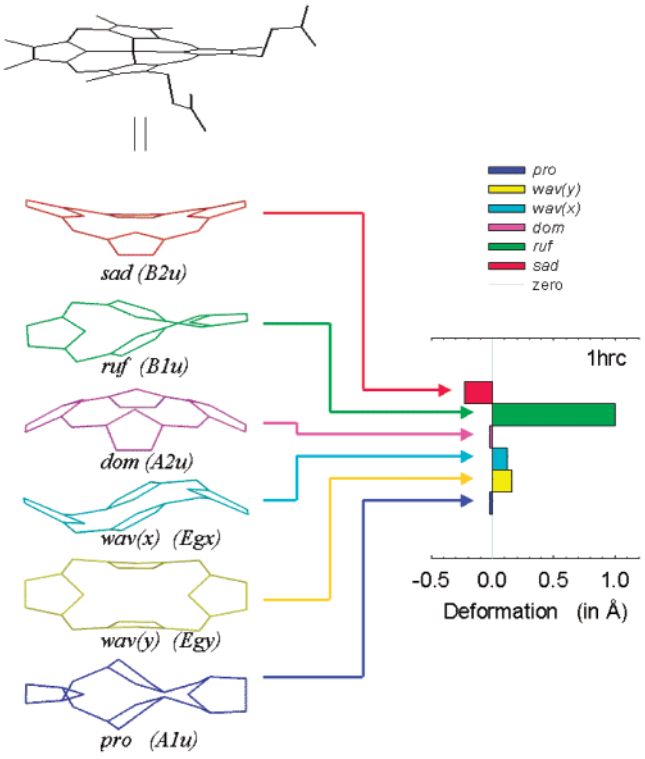

Figure 3. Lowest-frequency out-of-plane eigenvectors in the coordinate space for each of the normal deformations used in describing the nonplanar distortions of the macrocycle (printed with permission from J. A. Shelnutt).

have the same function, indicates a functional role for the distortion and an influence of proteins on nonplanar tetrapyrrole deformations.

Resonance Raman studies have shown that in solution nickel protoporphyrin is found in an equilibrium mixture of nonplanar and planar conformations. However, when the nickel protoporphyrin is bound to hemoglobin, it is only found in the planar conformation, even when the nickel is not coordinated to the proximal histidine.[22]

Numerous studies have shown that nonplanar distortions have a significant effect on the chemistries of tetrapyrrole complexes.[23] It has been suggested that the nonplanar deformations observed in photosynthetic proteins are responsible for the photophysical and redox properties of chlorophyll pigments.[24] Nonplanar porphyrins are easier to oxidize than planar porphyrins.[24−26] Excited-state lifetimes of porphyrins are influenced by nonplanar deformations,[25,27] as is the axial ligand affinity.[28]

We will show that MCR prevents coenzyme F430 from diepimerizing, thereby most likely modifying the chemistry of coenzyme. Furthermore, MCR moderates the degree of nonplanar deformations that occur when F430 is hydrogen bonded to MCR.

Experimental Section

Molecular Mechanics. The AMBER option of MacroModel v7.0X[29] was used with the default equations in all the molecular mechanical calculations. The parameters used to model the inorganic interactions were based on those we used in our previous calculations[15,16] and that were originally reported for complexes of low-spin and high-spin Ni(II) with polyamine ligands by Hancock and co-workers.[30,31] Convergence was considered complete when the gradient obtained was <0.001 kJ/mol. The crystal structures of MCR were downloaded from the Protein Data Bank.[32] Unless stated otherwise the $MCR_{ox1-silent}$ state (pdb code = 1mro) was used as the starting point for calculations. A hot-sphere of 8.00 Å around coenzyme F430 was used, and all atoms in this substructure were minimized without restriction. Two subsequent shells extending a further 2.00 Å each were constrained to their *x*, *y*, and *z* coordinates by a force constant of 100.00 kcal/mol·Å^2 for the first shell and a force constant of 200.00 kcal/mol·Å^2 for the second shell.

Conformational searches were conducted using the Monte Carlo (MC) torsional and molecular position variation method.[33,34] F430 was randomly rotated between 0 and 180° and randomly translated between 0 and 1.00 Å in each MC step.[35] The flexible dihedral angles of the side-chains of residues 120, 147, 153, 230, 330, 331, 333, 367, 396, and 443 were also randomly rotated between 0 and 180° in each MC step. There were 12 500 MC steps taken in each search. Structures within 50 kJ/mol of the lowest energy minimum were kept, and a usage directed method[36] was used to select structures for subsequent MC steps. Structures found in the conformational search were considered unique if the least-squares superimposition of equivalent non-hydrogen atoms found one or more pairs separated by 0.25 Å or more.

Normal-Coordinate Structural Decomposition. All the nickel(II) tetrapyrrole structures in the Cambridge Structure Database (CSD)[32] were downloaded and were analyzed by NSD as described in the literature[18,19] and as schematically represented in Figure 3. The NSD computational engine (http://jasheln.unm.edu/jasheln/content/nsd/NSDengine/docs_index.htm) was used for all decompositions. (Written by L.-S. Sun, W. Jentzen, and J. A. Shelnutt.)

Cluster Analysis. All the nickel(II) tetrapyrrole structures in the CSD (version 5.22) were downloaded, and the substituents (including hydrogens) were removed from the tetrapyrrole backbones. The atoms of every structure were renumbered such that the corresponding atoms of each ring were given the same number. To find all the symmetry-related conformations of these 20-membered ring systems, they were rotated 20-fold. Proximity matrixes were obtained by determining the pairwise distances between rings using

(22) Alden, R. G.; Ondrias, M. R.; Shelnutt, J. A. *J. Am. Chem. Soc.* **1990**, *112*, 691.
(23) Shelnutt, J. A.; Song, X. Z.; Ma, J. G.; Jia, S. L.; Jentzen, W.; Medforth, C. J. *Chem. Soc. Rev.* **1998**, *27*, 31−41.
(24) Barkigia, K. M.; Chantranupong, L.; Smith, K. M.; Fajer, J. *J. Am. Chem. Soc.* **1988**, *110*, 7566.
(25) Ravikanth, M.; Chandrashekar, T. *Struct. Bonding* **1995**, *82*, 107.
(26) Kadish, K. M.; Van Caemelbecke, E.; Dsouza, F.; Medforth, C. J.; Smith, K. M.; Tabard, A.; Guilard, R. *Inorg. Chem.* **1995**, *34*, 2984.
(27) Drain, C. M.; Kirmaier, C.; Medforth, C. J.; Nurco, D. J.; Smith, K. M.; Holten, D. *J. Phys. Chem.* **1996**, *100*, 11984.
(28) Othman, S.; Fitch, J.; Cusonovich, M. A.; Desbois, A. *Biochemistry* **1997**, *36*, 5499.
(29) Mohamadi, F.; Richards, N.; Guida, W.; Liskamp, R.; Lipton, M.; Caulfield, C.; Chang, G.; Hendrickson, T.; Still, W. *J. Comput. Chem.* **1990**, *11*, 440−467.
(30) McDougall, G.; Hancock, R.; Boeyens, J. *J. Chem. Soc., Dalton Trans.* **1978**, *1978*, 1438−1444.
(31) Hancock, R.; Dobson, S.; Evers, A.; Wade, P.; Ngwenya, M.; Boeyens, J.; Wainwright, K. *J. Am. Chem. Soc.* **1988**, *110*, 2788.
(32) Allen, F. H.; Kennard, O. *Chem. Des. Auto. News* **1993**, *8*, 31−37.
(33) Chang, G.; Guida, W. C.; Still, W. C. *J. Am. Chem. Soc.* **1989**, *111*, 4379−4386.
(34) Saunders, M.; Houk, K.; Wu, Y.-D.; Still, W.; Lipton, M.; Chang, G.; Guida, W. *J. Am. Chem. Soc.* **1990**, *112*, 1419.
(35) Bartol, J.; Comba, P.; Melter, M.; Zimmer, M. *J. Comput. Chem.* **1999**, *20*, 1549−1558.
(36) Shenkin, P.; McDonald, Q. *J. Comput. Chem.* **1994**, *15*, 899−916.

the root mean square (rms) deviation differences between corresponding external dihedral angles and the rms displacement between pairs of identically numbered atoms after optimal rigid-body superimposition. Cluster analysis was performed using the xcluster program.[36]

Results and Discussion

Magnitude of Saddling/Ruffling. A cluster analysis and a NSD were undertaken to establish how saddled/ruffled F430 and its diepimer are relative to other nickel(II) tetrapyrroles.

Cluster Analysis. Our cluster analysis of cobalt(III),[37] copper(II),[38] and nickel(II)[39] complexes containing the 14-membered tetra-aza macrocycles found that the macrocyclic ring structures were effectively separated according to their conformation by an agglomerative, hierarchical, single-link clustering method. Similar methods have also been used to group all the cobalt(III) porphyrins in the CSD on the basis of their nonplanar deformations.[40]

The latest version of the CSD (version 5.22) has 245 392 X-ray and neutron diffraction structures; of these 137 have a nickel(II) tetrapyrrole substructure. In cluster analysis, one attempts to group all the elements of interest into separate clusters in such a way that all the elements within a cluster are very similar to each other and dissimilar to elements in other clusters.[36,41] Cluster analysis can be used to group any elements with quantifiable properties. To perform a cluster analysis, one has to have a measure of difference between elements, a method of separating the items of interest, and some statistical measure for determining the clustering level, which is the most significant.

In all clustering methods, the first step is to set up a distance matrix that gives the distance from each element to every other element. Typical interconformational distance measures are the rms displacements of equivalent atoms in different molecules, which are taken after all the molecules have been optimally superimposed, and the rms differences of dihedral angles.

The most effective cluster analyses of the nickel(II) tetrapyrroles were those obtained after comparing the eight β-carbons, eight α-carbons, and four *meso*-carbons or the external torsion angles. Distance maps, cluster mosaics, and the separation ratios[36] were used to determine that at the best clustering level there are 40 clusters. Figure 4 shows the members of three of the largest clusters, clusters 4, 5, and 12. The cluster analysis has separated the planar structures (cluster 4), the ruffled ones (cluster 5), and the saddled ones (cluster 12). At the best clustering level there are 27 clusters with single members. One of them is the crystal structure of free diepimerized F430M[11] (CSD code = Kobcej). A second cluster analysis was performed in which F430s in MCR from *Methanobacterium thermoautotrophicum* (pdb codes = 1mro, 1hbn, 1hbm, 1hbo, and 1hbu), *Ms. barkeri*, and *Mp. kandleri* (pdb codes = 1e6y and 1e6v were added to the 137 structures with tetrapyrroloid substructures.

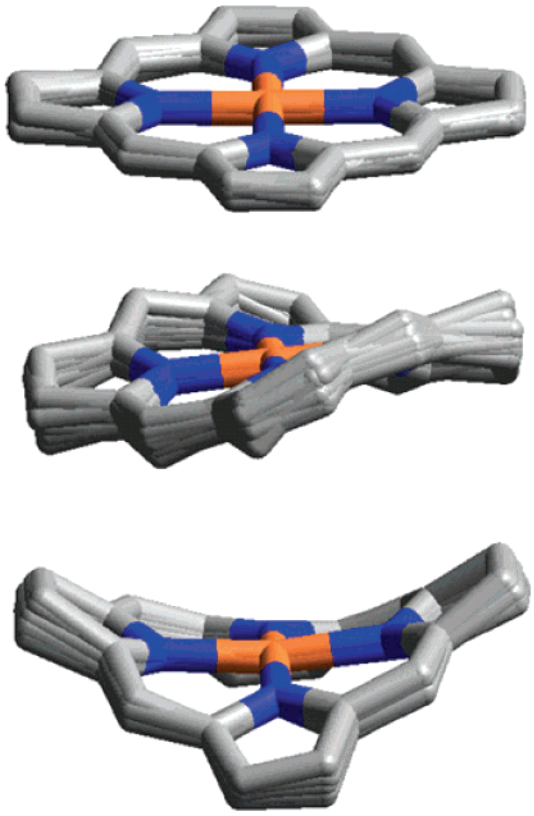

Figure 4. Overlap of all the structures in the three largest clusters at clustering level 98: cluster 4 (top), cluster 5 (middle), and cluster 12 (bottom).

At the best clustering level obtained in this analysis the *M. thermoautotrophicum* structures were all in the same cluster, and the *Ms. barkeri* and *Mp. kandleri* (pdb codes = 1e6y, r1e6ysf, 1e6v, and 1re6vsf) structures were in another cluster. Both clusters contained no tetrapyrrole structures. The cluster analysis was able to separate the tetrapyrrole structures on the basis of their nonplanar deformations. All the F430 structures were in clusters of their own; therefore, one can assume that the nonplanar deformations in F430 are different to those found in the tetrapyrroloid structures examined. This is not surprising given the reduced nature of the tetrahydrocorphinoid F430 ring system. On the basis of the cluster analysis we were able to establish which nickel(II) complexes had nonplanar deformations most similar to those observed in F430; this was done by examining the nearest neighbors of the clusters containing F430. However, it was not possible to quantify the degree of ruffling/saddling by using cluster analysis; therefore, NSD was used.

NSD. The method determines the out-of-plane distortions in terms of the equivalent distortions along the lowest-frequency normal coordinates of the porphyrin.[19] The predominant nonplanar deformations observed for the nickel(II) tetrapyrroles were the B2u (saddled) and the B1u (ruffled) normal deformations. Figure 5 shows the degree of ruffling and saddling, as determined by NSD analysis, of

(37) Cooper, C. G.; Zimmer, M. *Struct. Chem.* **1999**, *10*, 17−27.
(38) Bakaj, M.; Zimmer, M. *J. Mol. Struct.* **1999**, *508*, 59−72.
(39) Donnelly, M. A.; Zimmer, M. *Inorg. Chem.* **1999**, *38*, 1650−1658.
(40) Cullen, D. L.; Desai, L. V.; Zimmer, M.; Shelnutt, J. A. *Struct. Chem.* **2001**, *12*, 237−242.
(41) Torda, A.; van Gunsteren, W. *J. Comput. Chem.* **1994**, *15*, 1331−1340.

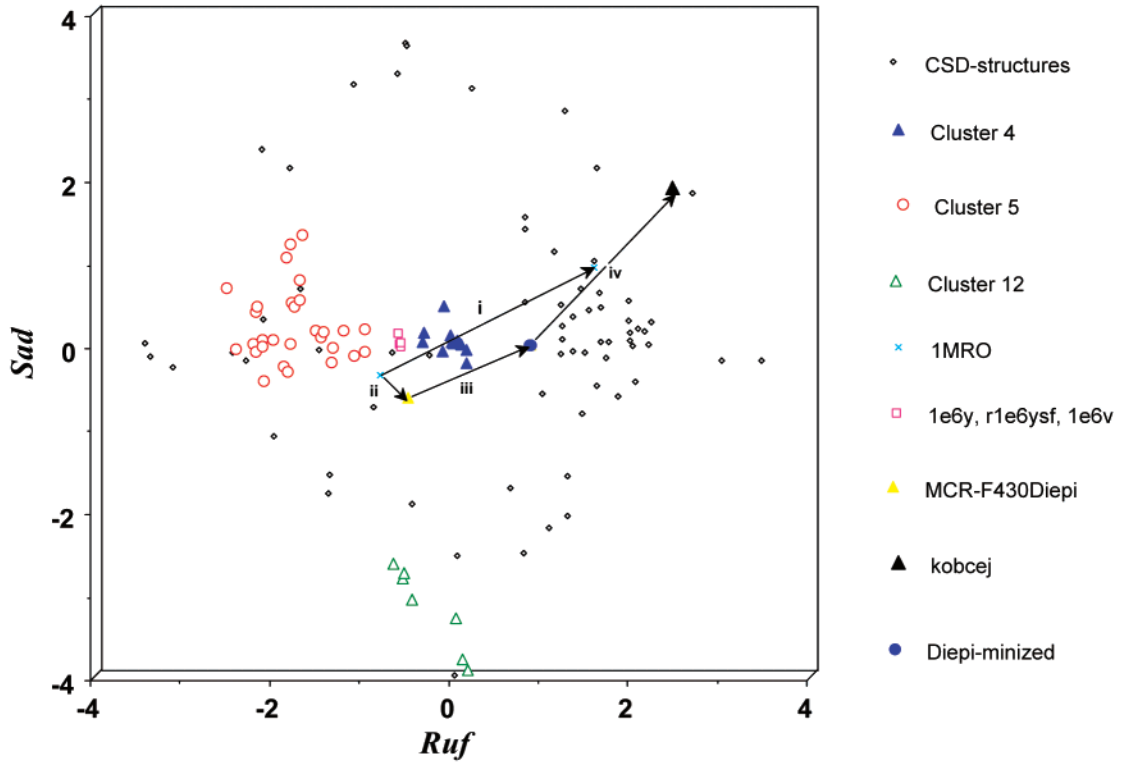

Figure 5. B2u (*sad*) and B2u (*ruf*) deformations of all the structures discussed in the paper. A 1-Å distortion means that the square root of the sum of the squares of the *z*-displacements from the mean plane is equal to one.[23] ◇: all the CSD structures, except those in clusters 4, 5, and 12. □: F430 in *Ms. barkeri* and *Mp. kandleri* MCR. Conformational changes shown are as follows: (i) F430 within MCR(1mro) to free F430, (ii) F430 within MCR to 12,-13-diepimerized F430 within the protein, (iii) 12,13-diepi-F430 to free 12,13-diepi-F430 minimized without a conformational search, and (iv) free 12,13-diepi-F430 minimized without a conformational search to the free 12,13-diepi-F430M solid-state structure.[43]

all the nickel tetrapyrroles in the CSD[32] and the tetrahydrocorphinoid F430 in the MCR crystal structures. The sign of the deformations is dependent on the molecular orientation chosen in the analysis. All the F430 structures and all the F430 model complexes were orientated the same way; therefore, this does not affect their analysis. However, since choosing a unique orientation for tetrapyrroles of widely varying structures is not simple and may even be impossible, no attempt was made to use the same molecular orientation. As a result the extent of the deformation is correct, but the signs of the deformations may not be consistent.

The B2u (saddled) and the B1u (ruffled) deformations of the structures in clusters 4, 5, and 12, obtained in the cluster analysis described above and depicted in Figure 4, are shown separately in Figure 5. The NSD analysis confirmed that the members of cluster 4 were planar (B1u and B2u $\approx$ 0), while those in cluster 5 were ruffled (B2u $\approx$ 0 and B1u ≈ -1 to -2), and those in cluster 12 were saddled (B1u $\approx$ 0 and B2u ≈ -3 to -4). Neighbors in the B1u versus B2u plot (Figure 5) are either in the same cluster or in neighboring clusters in the cluster analysis described above. According to the NSD analysis, the crystal structure of free diepimerized F430M[11] is highly distorted (CSD code = kobcej; B1u = 2.4359 and B2u = 1.8742) and is fairly similar to 2,3,12,-13-tetramethyl-4,14-dihydro-5,5,10,10,15,15,20,20-octaethylporphyrinogen-nickel(II)[42] (CSD code = hoghoa; B1u = 2.6592 and B2u = 1.8274), which like F430 is a very reduced tetrapyrrole. The two structures (hoghoa and kobcej) are also nearest neighbors in the cluster analysis described in the previous section.

If it were possible to use the same molecular orientation for all the tetrapyrroles, one would expect to find an even better correspondence between the NSD and the cluster analysis results. This sign ambiguity is responsible for the ring of structures seen in Figure 5.

Effect of MCR on the Nonplanar Deformations of F430. To determine the effect of the protein on the nonplanar deformations of the tetrahydrocorphinoid F430, molecular mechanics simulations and conformational searches of free cofactor F430 and cofactor F430 in MCR were carried out. The metal parameters used in our original study of F430[16] and modified for this study were derived by structure-based optimization of solid-state structures of tetrapyrroles and other macrocycles found in the CSD.[44,45] In essence these calculations interpolate the structure of an unknown complex on the basis of a set of parameters that were derived from fitting a number of crystal structures. One can therefore consider the resulting conformation as that of a complex in an averaged crystal lattice, not as solvated or in the gas phase.[44] If the complex being investigated differs significantly from the structures used to derive the parameters, the results will be of low quality. (Because of computational limitations

(42) Bonomo, L.; Solari, E.; Floriani, C.; Chiesi-Villa, A.; Rizzoli, C. *J. Am. Chem. Soc.* **1998**, *120*, 12972−12973.
(43) Kratky, C. F. A.; Pfaltz, A.; Krautler, B.; Jaun, B.; Eschenmoser, A. *J. Chem. Soc., Chem. Commun.* **1984**, *1984*, 1368−1371.
(44) Comba, P.; Zimmer, M. *J. Chem. Educ.* **1996**, *73*, 108−110.
(45) Zimmer, M. *Chem. Rev.* **1995**, *95*, 2629−2649.

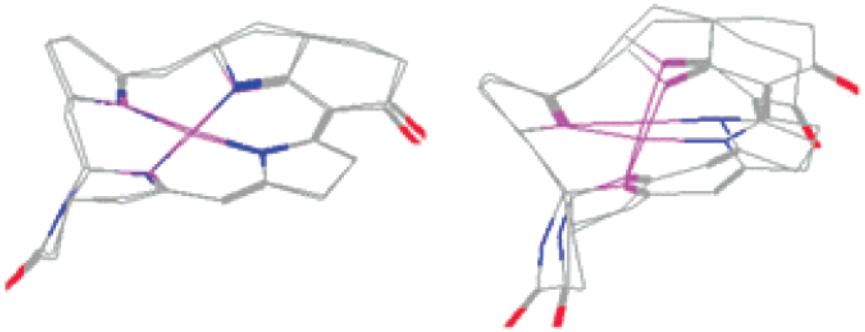

Figure 6. Left: overlap of the non-hydrogen F430 skeleton atoms in solid-state MCR (1mro) and the same atoms in F430 that were minimized within MCR. Right: overlap of the energy-minimized conformations of F430 within MCR and free F430.

Figure 7. Lowest-energy conformations of free F430 (left), F430 within MCR (center), and free 12,13-diepi-F430 (right).

all of MCR could not be modeled. Only the residues within an 8-Å sphere around coenzyme F430 were considered in our calculations. Given F430's size (Figure 1) this is a large sphere, and the calculations took weeks on a Linux cluster and the MERCURY supercomputer.)

Figure 5 shows that the conformation of the 12,13-diepi-F430M is more saddled/ruffled than most tetrapyrroles in the CSD and that it might therefore not be modeled very accurately. However, the force field and parameters have been shown[15] to model the structure, bond lengths, and angles of free 12,13-diepi-F430M. The ruffling, tetrahedrally distorted nickel and conformation was reproduced with slight deviations of the propionate and acetate side-chains as well as the cyclohexanone ring (D′). The rms deviation[46,47] of all the non-hydrogen atoms of the crystal and calculated F430 skeleton was 0.17 Å. The same rms deviation was obtained from the overlap of the non-hydrogen F430 skeleton atoms in solid-state MCR (1mro), and the same atoms for F430 were minimized within MCR (Figure 6 , left). Therefore, it can be assumed that the modified force field is a reliable predictor of the crystal-averaged structures of F430 complexes in and out of MCR.

The effect of the protein on the conformation of F430 can be seen by comparing the energy-minimized conformations of F430 within MCR and free F430. Figure 6, right, shows the overlap of the two structures. The rms deviation[46,47] of all the non-hydrogen skeleton atoms of the two F430s is 0.62 Å. The difference between the nonplanar deformations of the two conformations is also shown in Figure 5, line i. MCR constrains F430 to planarity (Figure 7 , center); when F430 is minimized outside of the protein it deforms from B1u = −0.819 and B2u = −0.387 to B1u = 1.5619 and B2u = 0.904 (Figure 5, line i). Similar behavior has been observed before; resonance Raman studies have shown that in solution nickel protoporphyrin exists as a mixture of planar and nonplanar conformations, while only the planar form is found when it is bound to hemoglobin.[22] X-ray absorption and resonance Raman spectroscopic studies have also shown that the conformation/axial coordination of F430 in MCR and free in solution is different,[48−50] supporting our structural conclusions.

12,13-Diepimeric Form of F430. Free coenzyme F430 is thermally unstable, as it first epimerizes to 13-epi-F430 and then in a second epimerization to 12,13-diepi-F430[10] (Figure 2). At thermodynamic equilibrium 4% of native F430, 8% of 13-epi-F430, and 88% of the most stable isomer 12,13-diepi-F430 are found. A parallel set of calculations to those described in the previous section were conducted with diepimeric F430 to establish how the MCR affects the diepimerization of cofactor F430. No major conformational changes were observed when the tetrahydrocorphin within MCR was graphically diepimerized at positions 12 and 13 and then minimized (Figure 5, line ii). The rms deviation between the non-hydrogen atoms in the two conformations is 0.33 Å with the majority of the deviation being in the two carbonyl oxygens and in ring C. 12,13-diepi-F430 undergoes substantial conformational changes when the surrounding protein is removed and the cofactor is minimized (Figure 5, line iii). However, the resultant conformation is not as deformed as the solid-state structure of 12,13-diepi-

(46) Kabsch, W. *Acta Crystallogr.* **1976**, *A32*, 922−923.
(47) Kabsch, W. *Acta Crystallogr.* **1978**, *A34*, 827−828.
(48) Shiemke, A. K.; Shelnutt, J. A.; Scott, R. A. *J. Biol. Chem.* **1989**, *264*, 11236.
(49) Shelnutt, J. A. *J. Phys. Chem.* **1989**, *93*, 6283.
(50) Shiemke, A. K.; Scott, R. A.; Shelnutt, J. A. *J. Am. Chem. Soc.* **1988**, *110*, 1645.

Table 1. Relative Energies of F430 and 12,13-D iepi in a Variety of Environs[a]

conformation	relative energy (kJ/mol)
F430 minimized in MCR (1MRO)	395
F430 removed from MCR and minimized	40.2
F430 diepimerized and minimized in MCR	846.3
F430 diepimerized, removed from MCR, and minimized	84.6
F430 diepimerized, removed from MCR, and ran a conformational search	0.0

[a] A single-point energy calculation was done of all F430 atoms without MCR (i.e., with the same atoms and connectivities in all cases).

F430M. To get from the conformation adopted by 12,13-diepi-F430 in MCR to that found in the solid-state structure of 12,13-diepi-F430M, a conformational search needs to be conducted. Table 1 lists the relative energies of the different forms of F430 shown in Figure 5 and discussed in this paper.

To be consistent all energies were calculated using all the coenzyme F430 atoms without considering any protein atoms. For example, F430 was minimized within MCR (using all residues within 8 Å of coenzyme F430), MCR was deleted, and the energy of F430 was calculated without minimization. The strain energy for 12,13-diepi-F430 within MCR was obtained by graphically diepimerizing F430 within MCR (pdb code = 1mro), minimizing within MCR, removing MCR, and calculating the energy of the 12,13-diepimer without minimizing. The strain energy obtained is extremely high because 12,13-diepi does not fit in the cavity that contains F430 in MCR.

Free 12,13-diepi-F430 has the lowest strain energy, and this is in agreement with the observation that 88% of this isomer is found at thermodynamic equilibrium. Although free 12,13-diepi-F430 has a lower energy conformation than free F430, the protein restraints exerted by MCR are responsible for F430 having a lower energy conformation than the 12,-13-diepimer in MCR. This also in agreement with experiment, which shows that none of the 12,13-diepimeric form is found in MCR. (These calculations are based on AMBER, modified with parameters determined by structure-based optimization of solid-state structures; therefore, we expect these calculations to produce relatively accurate averaged crystal lattice conformations, but we have less confidence in the relative energies of the conformations since energies were not used in the parametrization.) Figure 7 shows the conformation of F430 minimized within MCR (center), the conformation of F430 removed from MCR and minimized (left), and the lowest energy conformation of 12,13-diepi-F430. The planarity imposed upon F430 by MCR can be seen by comparing the relatively planar F430 found within MCR and the nonplanar deformed free F430. The difference in nonplanar deformations between free F430 and 12,13-diepi-F430 is also fairly obvious.

Translational and Rotational Freedom of F430 within MCR. F430 is noncovalently bound to MCR. On the basis of the similarity of the conformations of F430 found in the different crystal structures of MCR, it would seem that F430 does not have much conformational freedom in the protein. However, small changes, such as the 5° difference in the angle between the lactam ring and the pyrrole plane of the MCR-red1-silent and MCR-ox1-silent states, are observed. To find the translational and rotational freedom of F430 within MCR, a 12 500 step MC search was undertaken in which F430 was randomly rotated between 0 and 180° and randomly translated between 0 and 1.00 Å in each MC step. The flexible dihedral angles of the side-chains of all the residues within 5.00 Å of F430 were also varied between 0 and 180° in each MC step. Eight hundred and sixty-seven different conformations were found within 50 kJ/mol of the lowest energy conformation. In all conformations the surrounding residue side-chains have some conformational freedom, while the F430 macrocyle does not have much rotational or translational freedom.

Conclusion

The work described in this paper has shown that the protein in MCR has a significant structural effect on coenzyme F430 that influences the chemistry and reactivity of the enzyme. One of the ways in which MCR influences the chemistry at the nickel active site is by preventing coenzyme F430 from adopting the energetically more favorable 12,13-diepimeric conformer. Since the two diepimeric forms have differing reactivities, MCR is instrumental in determining the chemistry that occurs at the active site. It has been suggested that proteins are able to enforce unstable geometries, thereby producing an entatic state that can increase the reactivity of the active site. MCR does this by favoring F430 over 12,13-diepi-F430 and by moderating the nonplanar deformations F430 can adopt. It is known that redox potentials and axial ligand affinities are affected by the degree of nonplanarity present in tetrapyrroles. Therefore, that the protein environment (MCR) is capable of tuning the chemistry (redox potentials and axial ligand affinity) of the active site nickel ion and that computational studies such as this might be able to locate residues that can be mutated to moderate the extent of the nonplanar deformations found in F430, thereby changing its reactivity, are suggested.

Acknowledgment. This project was supported in part by NSF Grant CHE-0116435 as part of the MERCURY supercomputer consortium (http://mars.hamilton.edu). Acknowledgment is made to the Donors of the American Chemical Society Petroleum Research Fund for support of this research. M.Z. is a Henry Dreyfus Teacher-Scholar.

IC025950V